

Vol. 6, No. 1, October 2025, pp. 7-16, DOI: 10.59190/stc.v6i1.331

Design and optimization of square SRR metamaterialbased microstrip antenna for wideband biomedical sensing

Saktioto^{1,*}, Cici Yana Tasya Angraini¹, Yan Soerbakti¹, Ari Sulistyo Rini¹, Syamsudhuha², Sofia Anita³

¹Department of Physics, Universitas Riau, Pekanbaru 28293, Indonesia ²Department of Mathematics, Universitas Riau, Pekanbaru 28293, Indonesia ³Department of Chemistry, Universitas Riau, Pekanbaru 28293, Indonesia

ABSTRACT ARTICLE INFO

The continuous advancement in wireless biomedical technology necessitates the development of compact, high-performance antennas capable of operating across a wide frequency range. In this context, this study reports the design and optimization of a square split-ring resonator (SRR) metamaterial-based microstrip antenna to enhance bandwidth and gain characteristics for wideband biomedical sensing. The proposed metamaterial, composed of one to four square SRR unit cells, was modeled using copper patches on an FR-4 substrate with a dielectric constant of 4.3 and simulated in CST Studio Suite 2019 over a frequency range of 0.009 - 9 GHz. The electromagnetic behavior of the structure was analyzed through S-parameter characterization, and the Nicolson-Ross-Weir (NRW) retrieval method was applied to extract the effective constitutive parameters, including relative permittivity, relative permeability, and refractive index. The optimized four-cell SRR configuration demonstrated double-negative (DNG) characteristics, exhibiting a relative permittivity of -153.65, a relative permeability of -8.85, and a refractive index of -9.48, thereby confirming the negativeindex properties essential for enhanced electromagnetic field confinement and energy concentration. Integration of the optimized metamaterial into the microstrip antenna structure yielded significant performance improvement, achieving a return loss of -48.31 dB, bandwidth of 4.37 GHz, and gain of 2.23 dBi. These results substantiate that the square SRR metamaterial contributes to superior impedance matching and field localization, making the proposed antenna architecture highly promising for wideband biomedical sensing and potential internet of things (IoT) healthcare implementations.

Article history:

Received Sep 8, 2025 Revised Oct 24, 2025 Accepted Oct 25, 2025

Keywords:

Antenna Optimization Biomedical Application Microstrip Antenna SRR Metamaterial Wideband Sensing

This is an open access article under the <u>CC BY</u> license.



* Corresponding Author

E-mail address: saktioto@lecturer.unri.ac.id

1. INTRODUCTION

In recent years, the rapid evolution of wireless communication and biomedical monitoring technologies has intensified the demand for compact, efficient, and high-performance antennas capable of operating across wide frequency ranges. Among various antenna types, the microstrip patch has gained considerable attention due to its low profile, lightweight design, and ease of integration with microwave circuits, making it suitable for applications in aerospace, telecommunication, and biomedical systems [1-4]. Despite these advantages, conventional microstrip antennas exhibit inherent limitations such as narrow impedance bandwidth, low gain, and reduced radiation efficiency, which constrain their suitability for high-sensitivity and wideband operations [5, 6].

To overcome these challenges, the use of metamaterials has emerged as an effective approach to enhance antenna performance. Metamaterials are artificially structured composites that exhibit unique electromagnetic properties—such as negative permittivity (ϵ) and negative permeability (μ)—

not found in natural materials, thus enabling double-negative (DNG) characteristics [7-10]. These DNG properties facilitate superior field confinement, impedance matching, and miniaturization, which are advantageous for modern antenna design. The Split-Ring Resonator (SRR) is one of the most widely adopted metamaterial geometries, owing to its strong magnetic resonance and high controllability of electromagnetic wave propagation [11, 12]. The integration of SRR-based metamaterials into microstrip antennas has been reported to significantly improve gain, bandwidth, and directivity through enhanced electromagnetic coupling and resonant behavior [13-16].

Several studies have demonstrated the effectiveness of SRR geometries—such as circular, rectangular, and hexagonal configurations—in enhancing microstrip antenna performance across multiple frequency bands [17, 18]. However, the optimization of square SRR-based metamaterial structures remains relatively unexplored, particularly for wideband biomedical sensing, which requires high stability, sensitivity, and energy efficiency when interacting with biological tissues [19-22]. In biomedical, the antenna must not only achieve wideband response but also maintain high signal integrity and adaptability for physiological signal monitoring and IoT-based health systems [23, 24].

In this study, a square SRR metamaterial-based microstrip antenna is systematically designed and optimized to achieve superior wideband performance suitable for biomedical sensing. The metamaterial structure, consisting of one to four square SRR unit cells fabricated from copper on an FR-4 substrate, is analyzed using CST Studio Suite 2019 simulations in the frequency range of 0.009 – 9 GHz. The Nicolson–Ross–Weir (NRW) retrieval method is employed to extract the effective constitutive parameters of the metamaterial, including permittivity, permeability, and refractive index, to evaluate its DNG characteristics [25-27]. The optimized four-cell SRR configuration exhibits significant enhancement in return loss, bandwidth, and gain, demonstrating strong potential for integration into wideband biomedical and IoT-based sensing systems [28, 29].

2. RESEARCH METHOD

2.1. Simulation and Characterization of Metamaterial

The metamaterial used in this study is based on a square split ring resonator (SRR) configuration consisting of two concentric metallic rings. The structure was designed and simulated using CST Studio Suite 2019, and post-processing of the simulated S-parameters was conducted using MATLAB and Microsoft Excel. Copper was employed as the patch material, while FR-4 served as the dielectric substrate with a relative permittivity (ϵ_r) of 4.3. The initial design of the SRR metamaterial structure can be seen in Figure 1.

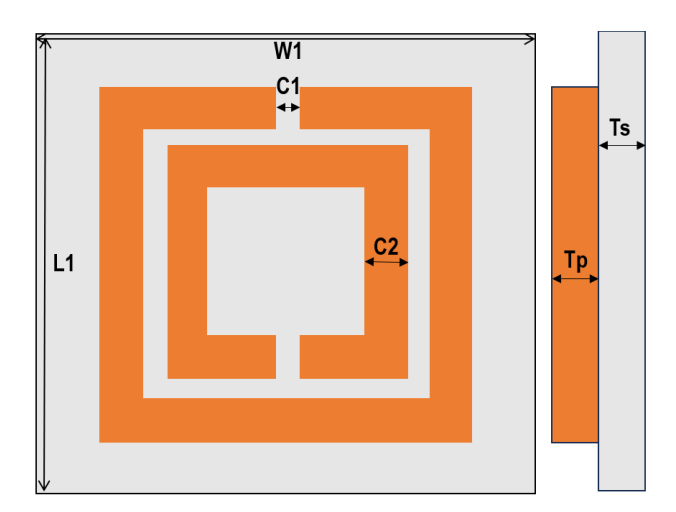


Figure 1. Front and side views of the square SRR metamaterial structure.

Figure 1 illustrates the front and side views of the proposed square SRR metamaterial design. The geometry demonstrates two concentric square copper rings separated by a narrow dielectric gap, mounted on the FR-4 substrate. This configuration allows strong magnetic resonance and field

localization, which are essential for achieving DNG behavior in the target frequency range. The radius size used is 3.5 mm and is the same for each cell variation. The geometric dimensions of the metamaterial structure can be seen in Table 1.

Table 1. Dimensional parameters of the SRR metamaterial structure.

| Parameter | Dimension (mm) | Parameter | Dimension (mm) |
|-----------|----------------|-----------|----------------|
| C1 | 0.43 | L1 | 7.4 |
| C2 | 0.6 | Ts | 1.6 |
| W1 | 2.14 | Tp | 0.035 |

To investigate the influence of the SRR cell count on electromagnetic properties, four variations were modeled, consisting of 1 to 4 SRR unit cells. The simulations were performed in the frequency range of 0.009-9 GHz to observe the double-negative (DNG) behavior in terms of permittivity (ε_r), permeability (μ_r), and refractive index (n).

Perfect Electric Conductor (PEC) and perfect magnetic conductor (PMC) boundary conditions were assigned to the model's input and output ports to define the excitation field and ensure accurate retrieval of scattering parameters (S_{11} and S_{21}). The Nicolson–Ross–Weir (NRW) method was used to derive the effective constitutive parameters from the simulated S-parameters, which were first converted from magnitude and phase into complex quantities. These parameters describe the intrinsic DNG characteristics of the metamaterial structure.

The simulated S-parameter data consist of the reflection coefficient (S_{11}) and transmission coefficient (S_{21}) obtained in both magnitude and phase domains. These quantities were subsequently converted into complex form using the following expressions [2]:

$$S_{11} = |S_{11}|e^{i\theta_{11}} \tag{1}$$

$$S_{21} = |S_{21}|e^{i\theta_{21}} \tag{2}$$

The electromagnetic characteristics of the metamaterial including the relative permittivity (ϵ_r), relative permeability (μ_r), and refractive index (n)—were determined using MATLAB implementation of the NRW retrieval method. The corresponding relations are expressed as follows [2]:

$$V_1 = S_{21} + S_{11} \tag{3}$$

$$V_2 = S_{21} - S_{11} \tag{4}$$

$$k = \frac{2}{jt_m} \frac{(1 - V_1)(1 + \Gamma_1)}{1 - \Gamma_1 V_1} \tag{5}$$

$$\mu_r = \frac{2}{jk_0t_m} \frac{1 - V_2}{1 + V_2} \tag{6}$$

$$\varepsilon_r = \frac{2}{jk_0 t_m} \frac{1 - V_1}{1 + V_1} \tag{7}$$

where, $k_0 = 2\pi f/c$ represents the free-space wave number, f is the operating frequency, and c denotes the speed of light in vacuum (3 × 10⁸ m/s). The parameter t_m corresponds to the propagation distance between the excitation input and output ports within the SRR metamaterial structure.

2.2. Design of Metamaterial Antenna

Following the characterization of the metamaterial, a microstrip antenna integrated with square SRR metamaterial cells was designed and optimized using CST Studio Suite 2019. The antenna consists of three main components: the substrate, the patch, and the ground plane. Both the patch and ground layers were made of copper, while the substrate utilized FR-4 material with a dielectric

constant of 4.3 and a thickness of 1.6 mm.A four-cell SRR configuration was selected for integration, as it exhibited the most stable DNG response during metamaterial characterization.

Figure 2 presents the front, back, and side views of the metamaterial antenna design. The structure illustrates the integration of the SRR array onto the microstrip patch, enhancing its resonant response through coupling between the SRR unit cells and the radiating surface. The antenna model underwent multiple optimization stages to refine its return loss, bandwidth, and gain.

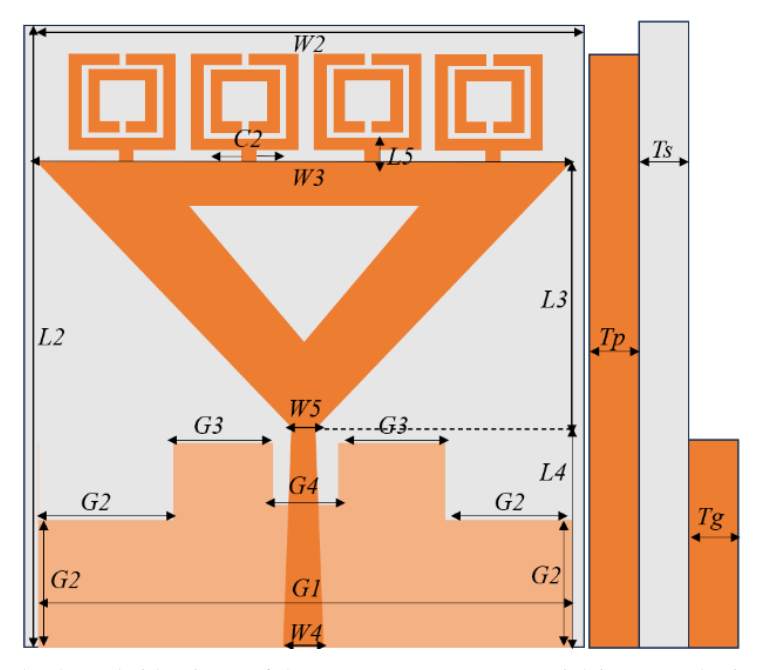


Figure 2. Front, back, and side views of the square SRR metamaterial-integrated microstrip antenna.

The geometric dimensions of the optimized antenna are summarized in Table 2. Each parameter was refined iteratively to achieve superior impedance matching, wideband operation, and improved gain performance.

| Parameter | Dimension (mm) | Parameter | Dimension (mm) |
|-----------|----------------|-----------|----------------|
| C2 | 1 | W4 | 2.14 |
| L2 | 25.65 | W5 | 1.27 |
| L3 | 14.54 | G1 | 29.6 |
| L4 | 11.11 | G2 | 7.4 |
| L5 | 0.82 | G3 | 5.43 |
| W2 | 29.6 | G4 | 3.94 |
| W3 | 29.6 | Tg | 0.035 |

Table 2. Geometrical dimensions of the metamaterial antenna.

3. RESULTS AND DISCUSSION

3.1. Metamaterial Structural Characteristics

The proposed square Split Ring Resonator (SRR) metamaterial was simulated with four different unit cell configurations to analyze its electromagnetic response and verify the presence of Double-Negative (DNG) characteristics [30]. The S-parameter data, specifically S_{11} (reflection) and S_{21} (transmission), were extracted from CST Studio Suite and processed using the Nicolson–Ross–Weir (NRW) retrieval method [31] to obtain the effective constitutive parameters: relative permittivity (ϵ_r), relative permeability (μ_r), and refractive index (n). The computed relationships between these parameters and frequency are presented in Figures 3 – 5.

As shown in Figure 3, the number of SRR cells strongly influences the dielectric properties of the metamaterial. The four-cell SRR configuration exhibits a significantly more pronounced negative permittivity response compared to other variations, with a peak resonance of $\epsilon_r = -153.65$ at 0.94 GHz. This result demonstrates enhanced electric field confinement and polarization within the metamaterial lattice, caused by the strong coupling between adjacent SRR elements [32]. The increased number of resonant units allows the structure to trap and manipulate more electromagnetic energy, confirming effective dielectric localization.

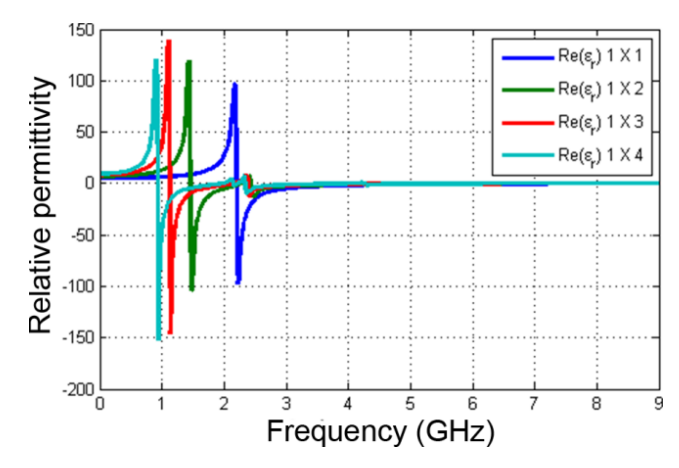


Figure 3. Effect of the number of SRR unit cells on the relative permittivity (\$\varepsilon\$) of the metamaterial structure.

The variation of relative permeability (μ_r) shown in Figure 4 reveals a similar trend. The four-cell SRR structure achieved the strongest magnetic resonance with a minimum μ_r value of -8.85 at 1.30 GHz. The simultaneous negativity of both ϵ_r and μ_r within overlapping frequency bands validates that the structure exhibits DNG behavior, which is critical for antenna miniaturization and performance enhancement in microwave applications [33]. The observed enhancement in magnetic response can be attributed to stronger induced magnetic flux within each resonant ring, increasing the overall electromagnetic coupling effect [34].

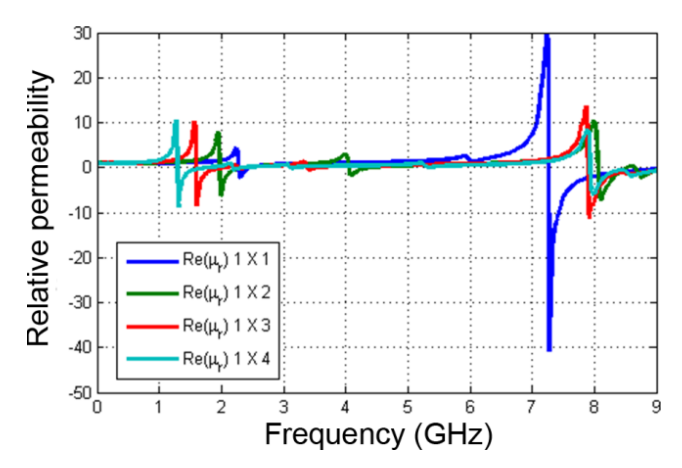


Figure 4. Effect of the number of SRR unit cells on the relative permeability (μr) of the metamaterial structure.

As depicted in Figure 5, the refractive index (n), calculated from ϵ_r and μ_r , also shows negative values over multiple frequency ranges. The single-cell SRR exhibits the most extreme negative refractive index (n = -12.23) at 2.28 GHz; however, the frequency of resonance gradually shifts as additional cells are introduced. This frequency shift results from mutual coupling and modification of the effective propagation path length within the metamaterial array [35]. The trend suggests that increasing the periodicity of SRR units enhances structural uniformity, improving stability and bandwidth at higher frequencies.

Overall, these findings confirm that increasing the number of SRR unit cells significantly affects the electromagnetic resonance characteristics of the metamaterial. The four-cell SRR configuration provides an optimal balance between electric and magnetic responses, thus being the most suitable structure for integration into a high-performance microstrip antenna system [36].

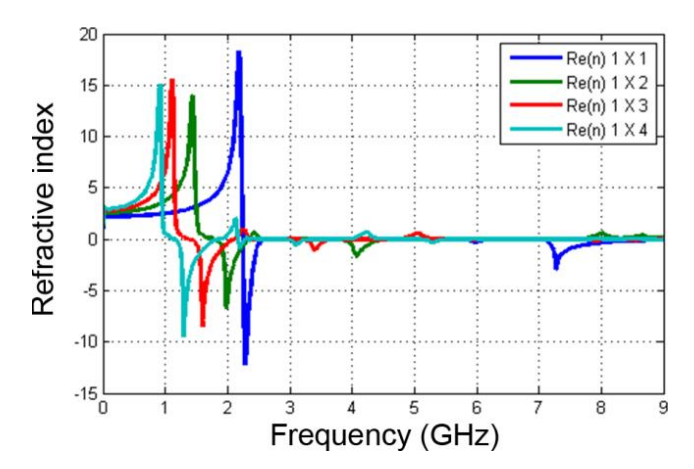


Figure 5. Variation of refractive index (n) with frequency for different SRR cell configurations.

3.2. Performance of the Metamaterial-Integrated Antenna

The microstrip antenna integrated with square SRR metamaterial structures was simulated to assess its radiation performance and impedance characteristics. Key parameters including return loss (S₁₁), Voltage Standing Wave Ratio (VSWR), gain, and radiation pattern were analyzed to evaluate the impact of SRR integration on antenna efficiency [37].

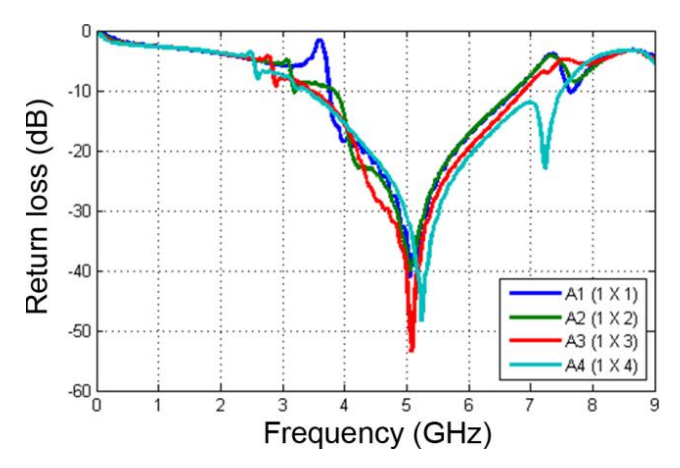


Figure 6. Comparison of return loss characteristics for microstrip antennas integrated with 1-4 SRR unit cells.

As shown in Figure 6, the integration of SRR metamaterial units leads to a notable improvement in return loss. The three-cell SRR antenna achieved the lowest return loss of -53.62 dB, indicating excellent impedance matching and minimal reflection loss. Similarly, the four-cell configuration maintained a low return loss of -48.31 dB, confirming efficient power transfer and reduced signal attenuation. These results align with previous findings showing that metamaterial superstrates and inclusions can significantly enhance antenna impedance bandwidth and radiation [38].

The VSWR results in Figure 7 show that all antenna designs maintain acceptable impedance matching within the standard range ($1 \le VSWR \le 2$). The four-cell SRR configuration achieved the widest operational bandwidth of 4.37 GHz, representing a substantial improvement compared to the conventional microstrip antenna without metamaterial integration [39]. The extended bandwidth is primarily attributed to multi-resonant interactions among the SRR elements, which introduce additional resonant modes and improve impedance continuity [40].

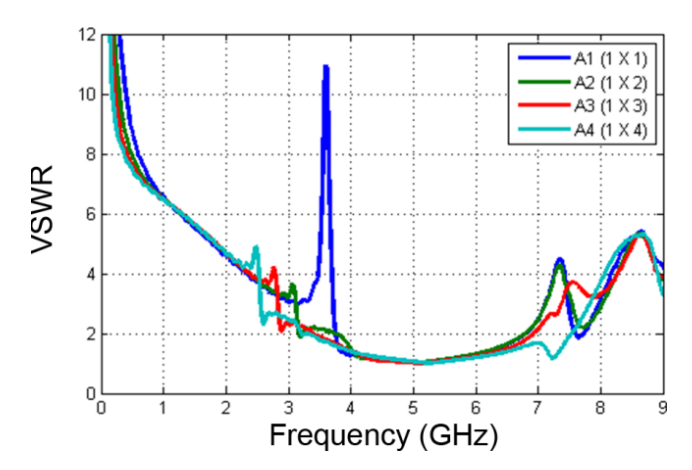


Figure 7. Comparison of VSWR characteristics for metamaterial-integrated microstrip antennas.

The gain behavior, as illustrated in Figure 8, shows consistent performance up to 2.69 GHz, after which the multi-cell configurations exhibit divergence due to inter-resonator coupling. The four-cell SRR antenna attained a maximum gain of 2.23 dBi, demonstrating that the metamaterial enhances radiation efficiency and field directivity by guiding electromagnetic waves through controlled coupling between the SRR lattice and the radiating patch [41]. These improvements confirm that the metamaterial structure effectively compensates for the inherent low-gain limitation of traditional microstrip antennas.

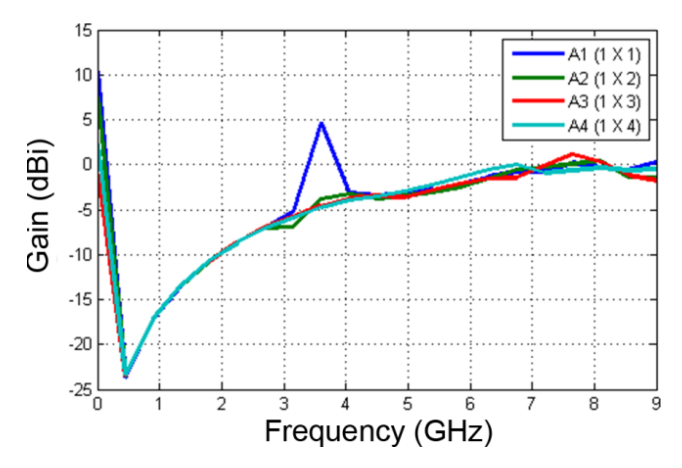


Figure 8. Gain characteristics of the microstrip antennas with different SRR configurations.

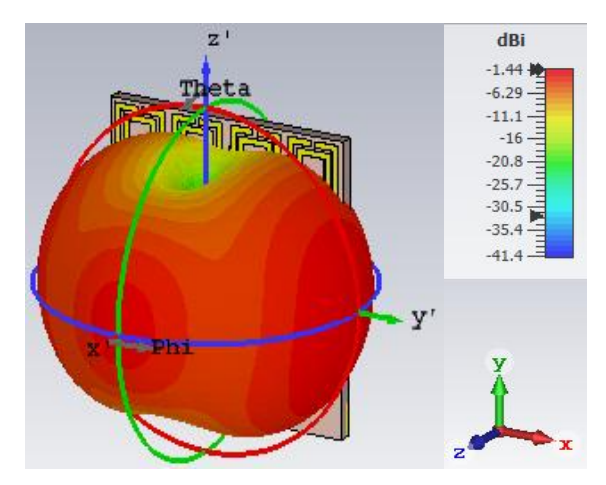


Figure 9. 3-dimensional radiation pattern of the optimized 4-cell SRR metamaterial-based microstrip antenna.

The radiation pattern of the optimized four-cell SRR antenna, shown in Figure 9, exhibits an omnidirectional distribution with the main lobe directed along the front axis. This pattern is particularly advantageous for biomedical sensing applications, where omnidirectional signal reception is essential for detecting physiological variations from different orientations [42]. The stable and symmetrical radiation pattern also reflects effective coupling between SRR units and the radiating element, ensuring consistent energy distribution and low distortion in near-field interactions.

3.3. Discussion

The overall results confirm that incorporating square SRR metamaterials into microstrip antenna design significantly enhances the antenna's electromagnetic and radiation performance [43]. The observed improvements in return loss, bandwidth, and gain are primarily due to the DNG properties of the metamaterial, which enable enhanced electromagnetic field localization and multiresonant operation [44].

Such characteristics allow the antenna to operate efficiently across a wide frequency band while maintaining compactness, structural simplicity, and stable radiation properties—features that are highly desirable for biomedical and IoT-based sensing devices [45]. The optimized four-cell SRR configuration therefore represents a promising and scalable platform for next-generation wideband biomedical sensors, offering improved signal reliability, low fabrication cost, and adaptability for flexible or wearable electronics applications [46].

4. CONCLUSION

This study successfully demonstrated the design, simulation, and optimization of a square Split Ring Resonator (SRR) metamaterial-based microstrip antenna for wideband biomedical sensing applications. The proposed metamaterial structure, comprising one to four square SRR unit cells, was characterized using the Nicolson–Ross–Weir (NRW) method, which confirmed the presence of Double-Negative (DNG) behavior. The optimized four-cell configuration exhibited strongly negative permittivity ($\epsilon_r = -153.65$) and permeability ($\mu_r = -8.85$), verifying its effective electromagnetic resonance properties.

Integration of the optimized metamaterial into the microstrip antenna significantly improved key performance parameters. The antenna achieved a return loss of –48.31 dB, bandwidth of 4.37 GHz, and gain of 2.23 dBi, accompanied by an omnidirectional radiation pattern ideal for biomedical sensing. These enhancements demonstrate that the DNG characteristics of the SRR metamaterial contribute to superior impedance matching, wideband operation, and radiation efficiency.

Overall, the results confirm that the square SRR metamaterial provides an efficient and scalable approach to improving microstrip antenna performance for biomedical and Internet-of-Things (IoT) applications. Future studies may extend this work toward reconfigurable, flexible, or miniaturized antenna systems for next-generation wearable healthcare devices.

ACKNOWLEDGMENTS

This research was supported by the RIIM program, funded by BRIN and LPDP under Contract 72/IV/KS/05/2023 and 10511/UN19.5.1.3/AL.04/2023. The authors sincerely thank both institutions for their continued support in the second-year funding (2025).

REFERENCES

- [1] Saravanan, S., Haimavathi, K. U., & Aafizaa, K. (2025). Biomedical antenna design: Micro strip patch antennas for wearable and implantable healthcare applications—A review. *Biomedical Materials & Devices*, 1–11.
- [2] Soerbakti, Y., Syahputra, R. F., Gamal, M. D. H., & Darwis, R. S. (2022). Improvement of low-profile microstrip antenna performance by hexagonal-shaped SRR structure with DNG metamaterial characteristic as UWB application. *Alexandria Engineering Journal*, **61**(6), 4241.
- [3] Saktioto, S., Siregar, F. H., Soerbakti, Y., Rini, A. S., Syamsudhuha, S., & Anita, S. (2024). Excellent integration of a multi-SRR-hexagonal DNG metamaterial into an inverted triangle top microstrip antenna for 5G technology applications at 3.5 GHz. *Przeglad Elektrotechniczny*, **100**.

- [4] Amalia, R., Defrianto, D., Soerbakti, Y., Asyana, V., & Abdullah, H. Y. (2024). Simulation and analysis of triangular structure metamaterial properties at microwave frequencies for medical sensor applications. *Science, Technology, and Communication Journal*, **5**(1), 15–20.
- [5] Islam, Z. U., Bermak, A., & Wang, B. (2024). A review of microstrip patch antenna-based passive sensors. *Sensors*, **24**(19), 6355.
- [6] Soerbakti, Y., Syahputra, R. F., Saktioto, S., & Gamal, M. D. H. (2020). Investigasi kinerja antena berdasarkan dispersi anomali metamaterial struktur heksagonal split ring resonator. *Komunikasi Fisika Indonesia*, **17**(2), 74–79.
- [7] Hakim, M. L., Alam, T., Soliman, M. S., Sahar, N. M., Baharuddin, M. H., Almalki, S. H., & Islam, M. T. (2022). Polarization insensitive symmetrical structured double negative (DNG) metamaterial absorber for Ku-band sensing applications. *Scientific Reports*, **12**(1), 479.
- [8] Defrianto, D., Soerbakti, Y., Syahputra, R. F., & Saktioto, S. (2020). Analisis kinerja antena berdasarkan pengaruh variasi kombinasi dan jarijari metamaterial heksagonal struktur split ring resonator. *Seminar Nasional Fisika Universitas Riau V (SNFUR-5)*, 5(1), 1–4.
- [9] Syahputra, R. F., Soerbakti, Y., & Saktioto, S. (2020). Effect of stripline number on resonant frequency of hexagonal split ring resonator metamaterial. *Journal of Aceh Physics Society*, **9**(1).
- [10] Gamal, M. D. H., Soerbakti, Y., Zamri, Z., Syahputra, R. F., & Saktioto, S. (2020). Investigasi karakteristik anomali indeks bias negatif metamaterial array struktur split ring resonator. *Seminar Nasional Fisika Universitas Riau V (SNFUR-5)*, **5**(1), 1–4.
- [11] Hasan, M. S., Islam, M. T., Mansor, M. F., Samsuzzaman, M., & Soliman, M. S. (2025). Split ring resonator-based triple band angle insensitive metamaterial absorber for EMI shielding and stealth applications in microwave frequency range. *Optics & Laser Technology*, **184**, 112546.
- [12] Soerbakti, Y., Saktioto, S., Dewi, R., & Rini, A. S. (2022). A review-Integrasi lapisan tipis ZnO pada aplikasi metamaterial sebagai wujud potensi sensor ultra-sensitif dan multi-deteksi. *Seminar Nasional Fisika Universitas Riau VII (SNFUR-7)*, **7**(1), 1–9.
- [13] Sifat, R., Faruque, M. R. I., Ramachandran, T., Abdullah, M., Islam, M. T., & Al-Mugren, K. S. (2024). SRR inspired inversion symmetry-shaped left-handed metamaterial with a high effective medium ratio for ASR and WLAN applications. *Heliyon*, **10**(4).
- [14] Soerbakti, Y., Defrianto, D., Rini, A. S., & Asyana, V. (2023). Performance analysis of metamaterial antennas based on variations in combination and radius of hexagonal SRR. *Science, Technology, and Communication Journal*, **4**(1), 1–4.
- [15] Soerbakti, Y., Gamal, M. D. H., Zamri, Z., Defrianto, D., & Syahputra, R. F. (2024). Negative refractive index anomaly characteristics of SRR hexagonal array metamaterials. *Science, Technology, and Communication Journal*, **4**(2), 63–68.
- [16] Soerbakti, Y., Rini, A. S., Astuti, B., Anita, S., Suyanto, H., & Rati, Y. (2024). Optimization of semiconductor-based SRR metamaterials as sensors. *Journal of Physics: Conference Series*.
- [17] Anitha, V. R., Palanisamy, S., & Hamam, H. (2024). Design and analysis of SRR based metamaterial loaded circular patch multiband antenna for satellite applications. *ICT Express*, **10**.
- [18] Saktioto, S., Soerbakti, Y., Rini, A. S., Astuti, B., & Rati, Y. (2024). Effectiveness of adding ZnO thin films to metamaterial structures as sensors. *Indonesian Physics Communication*, **21**.
- [19] Wang, J., Wang, R., Shen, Z., & Xue, Q. (2025). Microwave biosensors utilizing metamaterial enhancement: Design and application. *Nanotechnology and Precision Engineering*, **8**(1).
- [20] Saktioto, S., Soerbakti, Y., Rini, A. S., Astuti, B., Syamsudhuha, S., Anita, S., & Rati, Y. (2024). Extreme DNG metamaterial integrated by multi-SRR-square and ZnO thin film for early detection of analyte electrolyticity. *Przegląd Elektrotechniczny*, **100**.
- [21] Defrianto, D., Saktioto, S., Anita, S., Zahroh, S., and Soerbakti, Y. (2024). Perancangan dan simulasi antena telekomunikasi berdasarkan karakteristik metamaterial struktur lingkaran. *Prosiding Seminar Nasional Fisika Universitas Riau Ke-IX (SNFUR-9)*, **9**(1), 1002.
- [22] Amalia, R., Saktioto, S., and Soerbakti, Y. (2024). Simulasi dan analisis sifat metamaterial struktur segitiga pada frekuensi gelombang mikro untuk aplikasi sensor medis. *Prosiding Seminar Nasional Fisika Universitas Riau Ke-IX (SNFUR-9)*, **9**(1), 1001.
- [23] Musa, U., Shah, S. M., Majid, H. A., Mahadi, I. A., Rahim, M. K. A., Yahya, M. S., & Abidin, Z. Z. (2024). Design and implementation of active antennas for IoT-based healthcare monitoring system. *IEEE Access*, **12**, 48453–48471.

- [24] Rizwan, Y. F., Saktioto, S., and Soerbakti. Y. (2024). Perancangan struktur metamaterial segi empat pada frekuensi GHz untuk aplikasi antena mikro. *Prosiding Seminar Nasional Fisika Universitas Riau Ke-IX (SNFUR-9)*, **9**(1), 1004.
- [25] Angiulli, G. & Versaci, M. (2021). Retrieving the effective parameters of an electromagnetic metamaterial using the Nicolson-Ross-Weir method: An analytic continuation problem along the path determined by scattering parameters. *IEEE Access*, **9**, 77511–77525.
- [26] Defrianto, D., Saktioto, S., Rini, A. S., Syamsudhuha, S., Anita, S., & Soerbakti, Y. (2025). Exploration of Analyte Electrolyticity Using Multi-SRR-Hexagonal DNG Metamaterials and ZnO Thin Films. *Indonesian Journal of Electrical Engineering and Informatics (IJEEI)*, **13**(2).
- [27] Defrianto, D., Saktioto, S., Anita, S., Zahroh, S., Soerbakti, Y., and Emrinaldi, T. (2024). Analysis and modelling of the characteristics of telecommunication antennas utilising metamaterials with a circular structure. *Indonesian Physics Communication*, **21**(3), 233–238.
- [28] Saraswat, R. K. & Kumar, M. (2024). Implementation of the metamaterial multiband frequency reconfigurable antenna for IoT wireless standards. *IETE Journal of Research*, **70**(5), 4594.
- [29] Angraini, C. Y. T., Saktioto, S., and Soerbakti, Y. (2024). Rancangan dan simulasi metamaterial struktur persegi empat sebagai aplikasi antena. *Prosiding Seminar Nasional Fisika Universitas Riau Ke-IX (SNFUR-9)*, **9**(1), 1003.
- [30] Hussain, A., Dong, J., Abdulkarim, Y. I., Wu, R., Muhammadsharif, F. F., Shi, R., & Howlader, M. M. R. (2023). A double negative (DNG) metamaterial based on parallel double-E square split resonators for multi-band applications: Simulation and experiment. *Results in Physics*, 46.
- [31] Filbert, J. T., Dvorsky, M. R., Al Qaseer, M. T., & Zoughi, R. (2025). Unambiguous Determination of Complex Dielectric and Magnetic Materials Properties Using Multi-Length Nicolson-Ross-Weir Approach. *IEEE Transactions on Instrumentation and Measurement*, 74.
- [32] Bazgir, M. & Sheikhi, A. (2024). High Q-factor compact permittivity sensor based on coupled SRR-ELC metamaterial element and metasurfaces shield. *IEEE Sensors Journal*, **24**(4), 4424.
- [33] Kumari, R., Tomar, V. K., & Sharma, A. (2022). Miniaturization and performance enhancement of super wide band four element MIMO antenna using DNG metamaterial for THz applications. *Optical and Quantum Electronics*, **54**(9), 577.
- [34] Hou, X., Feng, X. R., & Wang, M. (2024). Enhancing electromagnetic shielding property and absorption coefficients via constructing. *Composites Science and Technology*, **257**, 110809.
- [35] Ahmed, A., Kumari, V., & Sheoran, G. (2023). Reduction of mutual coupling in antenna array using metamaterial surface absorber. *AEU-International Journal of Electronics and Communications*, **160**, 154519.
- [36] Menon, S. K. & Donelli, M. (2021). Development of a microwave sensor for solid and liquid substances based on closed loop resonator. *Sensors*, **21**(24), 8506.
- [37] Sathish, K., Saha, C., & Antar, Y. M. (2021). Varactor-controlled SRR-integrated frequency-reconfigurable multifunctional Vivaldi. *IEEE Antennas and Propagation Magazine*, **64**(3), 82.
- [38] Budarapu, S. K., Sunder, M. S., & Ramakrishna, B. (2023). Performance enhancement of patch antenna using RIS and metamaterial superstrate. *Progress In Electromagnetics Research C*, **130**.
- [39] Saadat Safa, M., & Tajik, S. (2025). Near-Field Microwave Sensing for Chip-Level Tamper Detection. Sensors, 25(13), 4188.
- [40] Ajewole, B., Kumar, P., & Afullo, T. (2022). I-shaped metamaterial using SRR for multi-band wireless communication. *Crystals*, **12**(4), 559.
- [41] Khan, M. S., Khan, S., Khan, O., Aqeel, S., Gohar, N., & Dalarsson, M. (2023). Mutual coupling reduction in MIMO DRA through metamaterials. *Sensors*, **23**(18), 7720.
- [42] Li, X. Y., Chen, L., & Cui, T. J. (2025). Contactless Electromagnetic Human Sensing for Biomedical and Healthcare Applications. *Progress In Electromagnetics Research*, **182**, 121.
- [43] Sediq, H. T. (2023). Miniaturized MIMO antenna design based on octagonal-shaped SRR metamaterial for UWB. *AEU-International Journal of Electronics and Communications*, **172**.
- [44] Sohi, A. K. (2025). Novel triangular-diamond fractal MIMO antenna with super-wideband capability for portable 5 G/IoT-driven wireless devices. *Physica Scripta*, **100**(7), 075528.
- [45] Sabban, A. (2024). Novel meta-fractal wearable sensors and antennas for medical, communication, 5G, and IoT applications. *Fractal and Fractional*, **8**(2), 100.
- [46] Ali, S. M., Noghanian, S., Khan, Z. U., & Alsulami, R. (2025). Wearable and flexible sensor devices: Recent advances in designs, fabrication methods, and applications. *Sensors*, **25**(5).